Molecular Pharmacology

Original article

Title

Investigation of the Endoplasmic Reticulum Localization of UDP-Glucuronosyltransferase 2B7
with Systematic Deletion Mutants

Yuu Miyauchi*, Sora Kimura*, Akane Kimura, Ken Kurohara, Yuko Hirota, Keiko Fujimoto,
Peter I. Mackenzie, Yoshitaka Tanaka, and Yuji Ishii

Division of Pharmaceutical Cell Biology, Graduate School of Pharmaceutical Sciences, Kyushu
University, Fukuoka, Japan (Y.M., A.K., K.K., Y.H., K.F., Y.T.)
Laboratory of Molecular Life Sciences, Graduate School of Pharmaceutical Sciences, Kyushu
University, Fukuoka, Japan (Y.M., S.K., Y.I.)
Department of Clinical Pharmacology, Flinders Medical Centre and Flinders University, Adelaide,
Australia (P.I.M.)

*; Equally contributed

Running Title Page

Running Title: Lack of an export signal retains UGT2B7 in the ER

Correspondence: Yuu Miyauchi, Division of Pharmaceutical Cell Biology, Graduate School of Pharmaceutical Sciences, Kyushu University, 3-1-1 Maidashi, Higashi-ku, Fukuoka 812-8582, Japan, Tel.: +81-92-642-6619; Fax: +81-92-642-6619; E-mail: ymiyauchi@phar.kyushu-u.ac.jp or Yuji Ishii, Laboratory of Molecular Life Sciences, Graduate School of Pharmaceutical Sciences, Kyushu University, 3-1-1 Maidashi, Higashi-ku, Fukuoka 812-8582, Japan, Tel.: +81-92-642-6586; Fax: +81-92-642-6588; E-mail: ishii@phar.kyushu-u.ac.jp

Number of text pages: 26

Number of tables: one

Number of figures: eight

Number of references: 49

Abstract: 242 words (Max 250)

Introduction: 676 words (Max 750)

Discussion: 828 words (Max 1500)

Abbreviations

CD4, T-cell surface glycoprotein CD4; CNX, calnexin; CYP and P450, cytochrome P450; ER, endoplasmic reticulum; ERAD, endoplasmic reticulum-associated degradation; HLM, human liver microsomes; HRP, horseradish peroxidase; PCR, polymerase chain reaction; UGT, UDP-glucuronosyltransferase

ABSTRACT

UDP-Glucuronosyltransferase (UGT) plays an important role in the metabolism of endogenous and exogenous compounds. UGT is a type I membrane protein, and has a di-lysine motif (KKXX/KXKXX) in its C-terminal cytoplasmic domain. Although a di-lysine motif is defined as an endoplasmic reticulum (ER) retrieval signal, it remains a matter of debate whether this motif functions in the ER localization of UGT. To address this issue, we generated systematic deletion mutants of UGT2B7, a major human isoform, and compared their subcellular localizations with that of an ER marker protein calnexin (CNX), using subcellular fractionation and immunofluorescent microscopy. We found that although the di-lysine motif functioned as the ER retention signal in a chimera that replaced the cytoplasmic domain of CD4 with that of UGT2B7, UGT2B7 truncated mutants lacking this motif extensively colocalized with CNX, indicating di-lysine motif independent ER retention of UGT2B7. Moreover, deletion of the C-terminal transmembrane and cytoplasmic domains did not affect ER localization of UGT2B7, suggesting that the signal necessary for ER retention of UGT2B7 is present in its luminal domain. Serial deletions of the luminal domain, however, did not affect the ER retention of the mutants. Further, a cytoplasmic and transmembrane domain-deleted mutant of UGT2B7 was localized to the ER without being secreted. These results suggest that UGT2B7 could localize to the ER without any retention signal, and lead to the conclusion that the static localization of UGT results from lack of a signal for export from the ER.

Introduction

In eukaryotic cells, the secretory pathway is a conserved biosynthetic transport route for secreted proteins and proteins localized in each organelle constituting the pathway. All of the proteins transported in this pathway are synthesized in the endoplasmic reticulum (ER) and delivered to their destinations by vesicular transport (Gomez-Navarro and Miller, 2016). In general, two strategies are believed to be necessary for ER proteins to reside in the ER, *i.e.*, 1) retention; elimination from the vesicles involved in anterograde transport and 2) retrieval; capture and return of the escaped ER residents by coat protein I complex (COPI) vesicles (Barlowe and Helenius, 2016; Teasdale and Jackson, 1996). The mechanism of retention remains controversial, but the second mechanism is more established, and known as motif-based retrieval to the ER. The carboxyl-terminal tetra-peptide KDEL and HDEL are necessary for ER soluble proteins to be retrieved by COPI in mammals and yeast, respectively (Munro and Pelham, 1987; Pelham, 1988). The C-terminal di-lysine motif (KKXX/KXKXX) is also defined as a retrieval signal for type I membrane residents in the ER (Gaynor et al., 1994; Jackson et al., 1993; Nilsson et al., 1989).

UDP-Glucuronosyltransferase (UGT) is one of the major drug-metabolizing enzymes catalyzing glucuronidation, and 22 isoforms have been identified so far. Among them, 19 isoforms have been reported to be involved in glucuronidation in human (Rowland et al., 2013). Most research on UGT is focused on its enzymatic activity, because the enzyme is involved in the metabolism of the second largest number of drugs, following cytochrome P450 (P450 or CYP) (Evans and Relling, 1999). However, UGT is also a model for studies on ER localization. UGT is a typical type I membrane protein, with most of the protein, including the substrate-binding site, on the luminal side of the ER membrane. Only a single transmembrane helix exists in its C-terminal region, followed by about 20 residues facing the cytosol (cytoplasmic tail). UGT has a di-lysine motif at its C-terminus (Fig. 1) (Harding et al., 1987; Iyanagi et al., 1986; Radominska-Pandya et al., 1999; Shepherd et al., 1989), and its functions were well examined. The di-lysine motif of UGT was transplanted onto the end of the cytoplasmic tail of plasma membrane proteins, *e.g.* CD4, CD8, and ErbB2, which altered their localization from the plasma membrane to the ER (Jackson et al., 1990; Kinosaki et al., 1993). These studies were enough to believe that the C-terminal motif was a major driving force for UGT localization in the ER. However, there is also evidence that UGT is able to localize in the ER in a di-lysine motif-independent manner. Deletion mutants of rat UGT2B1, human UGT1A6 and other isoforms lacking the cytosolic tail and transmembrane region are still retained in the ER (Jackson et al., 1993; Meech et al., 1996; Ouzzine et al., 1999). In our recent study, we also obtained similar results with UGT2B7. UGT2B7 is an important human isoform catalyzing the metabolism of a huge number of clinical drugs, *eg*. morphine and zidovudine (Rowland et al., 2013). In addition, UGT2B7 is also involved in the glucuronidation of endogenous compounds such as fatty acids, and steroids (Bock, 2012;

4

Bowalgaha et al., 2007). Further, there are reports that UGT can localize to other organelles beside the ER, *e.g.* mitochondria, Golgi apparatus, and plasma membrane (Chowdhury et al., 1985; Menard et al., 2013; Radominska-Pandya et al., 2005; Ziegler et al., 2015). A growing number of studies demonstrate that the ER can make contact with other organelles, exchange membrane composition, and function as a central hub for organelle interaction (Schrader et al., 2015; Shim, 2017). Thus, elucidating the mechanisms by which UGT localizes to the ER is expected to lead to new insights into drug metabolism.

To address this issue, in the present study, we used two separate procedures: cellular fractionation and immunocytochemistry to ascertain the role of the di-lysine motif in UGT2B7 localization. We then generated systematic deletion mutants lacking not only the C-terminal transmembrane and/or cytoplasmic domains, but also one or several sections of the ER luminal domain of UGT2B7 to look for another ER retention sequence.

Materials and Methods

Materials. Synthetic oligonucleotides were purchased from Fasmac (Kanagawa, Japan). Restriction enzymes and other DNA-modifying enzymes were from Takara Bio (Shiga, Japan). Glass products for immunofluorescence microscopy were from Matsunami Glass (Osaka, Japan). Pooled human liver microsomes (HLM, prepared from 50 donors) were from Corning® Gentest (Woburn, MA). All other reagents were of the highest quality commercially available.

Subcloning of UGT2B7 and its mutants into a bacuroviral vector. Recombinant baculoviruses coding UGT2B7 wild-type (WT), ΔCT (Δ511-529), ΔTM (Δ493-529), and human calnexin (CNX) were prepared using Bac-to-Bac® Baculovirus Expression System (Life Technologies, Carlsbad, CA) as described previously (Miyauchi et al., 2015). ΔDM (Δ525-529) was generated by polymerase chain reaction (PCR) using pFastBac1-WT as a template, KOD-Plus-Neo DNA polymerase (Toyobo Life Science, Osaka, Japan), and the following a pair of primer: sense, 5'-GG<u>GGTACC</u>GGGATGTCTGTTAAATGG-3'; anti-sense, 5'-GG<u>GGTACC</u>TTACTTTGCTTTTCTAGCAAA-3'(underline, *Kpn*I sites). Thermal cycle parameters were as follows: initial denaturation, 94°C, 2 min; cycling step (×40 rounds), 98°C, 10 s; 52°C, 30 s; 68°C, 1 min; hold, 4°C. The PCR product was purified with FastGene Gel/PCR Extraction Kit (NIPPON Genetics, Tokyo, Japan) and subcloned into pFastBac1 vector using *Kpn*I-sites. Hemagglutinin epitope tag (HA-tag) was introduced into the C-terminus of WT to yield WT-HA by QuickChange site-directed mutagenesis. Primers were designed by Agilent QuickChange Primer Design Program (https://www.genomics.agilent.com/primerDesignProgram.jsp), and non-tagged pFastBac1 construct was used as a template. Sequences of the primers were as follows: sense, 5'-GCTAGAAAAGCAAAGAAGGGAAAAAATGAT<u>TACCCATACGATGTTCCAGATTACGCT</u>TAGGGTACCAAGCTTG-3'; anti-sense, 5'-CAAGCTTGGTACCCTA<u>AGCGTAATCTGGAACATCGTATGGGTA</u>ATCATTTTTTCCCTTCTTTGCTTTTCTAGC-3' (underline, coding HA-tag). Thermal cycle parameters were " a two steps cycle" as follows: initial denaturation, 94°C, 2 min; cycling step (×20 rounds), 98°C, 10 s; 68°C, 4 min; hold, 4°C. Template vectors were digested by *Dpn*I treatment, and the reaction mixtures were utilized in transformation with Competent Quick DH5α (Toyobo Life Sciences). Further deletion mutants with HA-tag (Δ1-HA to Δ5-HA) were also prepared by site-directed mutagenesis using pFastBac1-WT-HA construct as a template. Primers are listed in supplemental Table S1. Mutagenesis was carried out under the two step cycling above mentioned. The nucleotide sequences of the constructs were confirmed by an ABI 3130xl Genetic analyzer, using a BigDye® Terminator v3.1 Cycle Sequencing Kit (Life Technologies). Recombinant pFastBac1 were transfected into competent *Escherichia coli* DH10Bac™ strain (Life Technology). After blue/white selection, positive single clone was picked up and cultured to obtain recombinant

bacmid, a part of baculoviral DNA, according to the user's manual.

Culture of Sf9 cells and preparation of microsomes. Sf9 insect cells were cultured under the conditions in our previous study with slight modifications (Ishii et al., 2014). In short, the cells were grown in a 500 ml plastic Erlenmeyer flask (Corning, St. Lowell, MA) containing Sf-900II medium (Life Technologies) supplemented with 5% fetal bovine serum (FBS) and 10 μg/ml gentamycin. To obtain recombinant baculovirus, Sf9 cells (2×10^7 cell) were seeded in a 175 cm^2 t-flask (Thermo Scientific, Rockford, IL), and then transfected with recombinant bacmids with Cellfectin®II reagent (Life Technologies) diluted with Sf-900II medium in the absence of FBS or antibiotics. After 5 hr incubation, the medium was replaced with fresh one, and the cells were cultured for seven days. The cells were pelleted by low-speed centrifugation, and the supernatant was collected as primary (P1) virus. The pelleted cells were re-suspended in 10 mL phosphate-buffered saline (PBS), and an aliquot of the suspension was mixed with the same volume of 2×SDS-polyacrylamide gel electrophoresis (SDS-PAGE) sampling buffer (125 mM Tris-HCl (pH 6.8), 4% SDS, 20% glycerol, 0.006% bromophenol blue, 10% 2-mercaptoethanol) to prepare whole cell lysate for confirmation of target protein expression. Titer of the recombinant baculovirus was determined using a BacPAK™ qPCR Titration Kit (Clontech, Mountain View, CA). Baculoviral titer was amplified by several rounds of transfection until a titer of over 1.0×10^7 plaque-forming units/ml was obtained. For expression of recombinant enzymes, Sf9 cells (2×10^6 cells/ml, 200 ml) were infected with recombinant baculovirus, and cultured for 48 hr. Microsomes were prepared from them according to the protocols described previously (Ishii et al., 2014).

Construction of recombinant mammalian expression vectors. cDNA of CD4 was purchased from Ori-Gene technologies (Rockville, MD) and amplified by PCR with a pair of primer: sense, 5'-CCG<u>CTCGAG</u>ACAATGAACCGGGGAGTCCCTTTTAGG-3' (sense primer A; underline, *Xho*I site); anti-sense, 5'-CGG<u>GGTACC</u>TCAAATGGGGCTACATGTCTTC-3' (underline, *Kpn*I site). The PCR product was digested with *Xho*I and *Kpn*I and subcloned into the pcDNA3.1/hygro (−) vector for transient expression in COS-1 cells. A deletion mutant of CD4 lacking transmembrane and cytoplasmic domains (CD4 ΔTM) was generated by QuickChange site-directed mutagenesis with a pair of primers: sense, 5'-CCACCCCGGTGCAGCCATGAGGTACCAAG-3'; anti-sense, 5'-CTTGGTACCTCATGGCTGCACCGGGGTGG-3'. The mutagenesis was conducted with the pcDNA3.1/hygro (−)_CD4 construct as a template under the following thermal cycle conditions: initial denaturation, 94°C, 2 min; cycling step (×25 rounds), 98°C, 10 s; 52°C, 30 s; 68°C, 4 min; extra extension, 68°C, 5 min; hold, 4°C. The PCR product was digested with *Dpn*I, and utilized for transformation. A chimeric protein of CD4 (CD4-UGT), which replaced the cytoplasmic domain of CD4 with that of UGT2B7 was generated by sequential PCRs. Each PCR

product was utilized as a template in the next round of PCR. Pairs of primers used in each round of PCR are listed below: 1st round sense, sense primer A; 1st round anti-sense, 5'-GAAACAAAACAGACAACATTT**GAAGAAGATGCCTAGCCC**-3' (bold, sequence coding the end of transmembrane region of CD4); 2nd round sense, 5'-CCG<u>CTCGAG</u>ACAATGAACC-3' (sense primer B, underline, *Xho*I site); 2nd round anti-sense, 5'-TTCTTTGCTTTTCTAGCAAACTTCCAGAAACAAAACAGACAACATTTG-3'; 3rd round sense, sense primer B; 3rd round anti-sense, 5'-GG<u>GGTACC</u>CTAATCATTTTTTCCCTTCTTTGCTTTTCTAGCAAAC-3' (underline, *Kpn*I site). Products of the 3rd round PCR were subcloned into the pcDNA3.1/hygro (−) vector using *Xho*I-*Kpn*I sites. Addition of a HA-tag to the C-terminus and alanine mutation of the di-lysine motif of CD4-UGT were conducted by site-directed mutagenesis with pairs of primers: sense for addition of the HA-tag, 5'-GCTAGAAAAGCAAAGAAGGGAAAAAATGAT<u>TACCCATACGATGTTCCAGATTACGCT</u>TAGGGTACCAAGCTTA-3' (underline, HA-tag); anti-sense for addition of the HA-tag, 5'-TAAGCTTGGTACCCTA<u>AGCGTAATCTGGAACATCGTATGGGTA</u>ATCATTTTTTCCCTTCTTTGCTTTTCTAGC-3' (underline, HA-tag); sense for alanine mutation of the di-lysine motif, 5'-GTTTCTGGAAGTTTGCTAGAAAAGCAAAG<u>GC</u>GGGA<u>GCA</u>AATGATTAGGGTACCAAGCTTAAGTTTA-3' (underline, alanine mutations); anti-sense for alanine mutation of the di-lysine motif, 5'-TAAACTTAAGCTTGGTACCCTAATCATT<u>TGC</u>TCC<u>CGC</u>CTTTGCTTTTCTAGCAAACTTCCAGAAAC-3' (underline, alanine mutations). Mutagenesis was conducted with pcDNA3.1/hygro_CD4-UGT as template in a two step cycle. PCR products were treated with *Dpn*I and utilized for transformation to obtain the desired constructs. DNA of UGT2B7 WT and WT-HA were subcloned from pFastBac1 to pcDNA3.1/hygro (−) vector using *Kpn*I-sites. The HA-tag was also added to the C-terminal end of ΔDM, ΔCT, and ΔTM by site-directed mutagenesis using pFastBac1 constructs as templates. Primers utilized in the mutagenesis are listed in supplemental Table S2, and amplification was carried out in a two-cycle step as mentioned above. After HA-tag addition, cDNAs of ΔDM-HA, ΔCT-HA, and ΔTM-HA were subcloned into pcDNA3.1/hygro (−) as done with WT-HA. In addition, mammalian constructs coding UGT2B7 Δ1-Δ11 with HA-tag were generated by two-cycle step mutagenesis. Primers and templates utilized for preparing Δ1-Δ5 and Δ6-Δ11 are listed in supplemental Table S3, and S4, respectively. After *Dpn*I treatment, reaction mixtures were used for transformation of E. *coli*. Nucleotide sequences were checked according to the protocol described above.

Culture of COS-1 cells and transfection of mammalian expression vector. COS-1 cells were grown in Dulbecco's modified Eagle medium (DMEM) containing high glucose (Wako Pure

Chemical, Osaka, Japan) and 10% FBS. For immunoblotting, cells were seeded in 35 mm dishes the day before transfection, and pcDNA3.1 vectors (2 µg) were transfected with FuGENE6 (Promega, Madison, WI) according to the manufacturer's protocol. Twenty four hours after transfection, the cells were lysed in lysis buffer, 20 mM Tris-HCl (pH 7.4) containing 150 mM NaCl, 1% Triton X-100, 10% glycerol, and protease inhibitor cocktail (Nacalai Tesque, Kyoto, Japan), and sonicated to prepare whole cell lysates. For immunofluorescence staining, cells were plated onto 13-mm coverslips the day before transfection. The amount of transfected pcDNA3.1 was 1 µg with FuGENE6 as a transfection reagent, and immunofluorescence staining was performed 24 hr after transfection.

Immunoblotting. Proteins separated by SDS-PAGE were electroblotted on to a polyvinylidene difluoride (PVDF) membrane (Merck Millipore, Burlington, MA). UGT2B7 was detected either by goat anti-mouse low p*I* form UGT antibody (Mackenzie et al., 1984) or rabbit anti-HA-tag antibody (Sigma Aldrich, St. Louis, MO). Rabbit anti-CNX (GeneTex, Irvine, CA) and mouse anti-β-actin (Sigma Aldrich) were purchased from the sources indicated. The primary antibodies were diluted 2,000-fold when used. Immunochemical detection was conducted either with horseradish peroxidase (HRP)-conjugated secondary antibodies, HRP-rabbit anti-goat IgG (MP Biomedicals, Santa Ana, CA) or HRP-donkey anti-rabbit IgG (GE Healthcare, Little Chalfont, UK). The secondary antibodies were diluted 10,000-fold in use. EzWestLumi plus (ATTO, Tokyo, Japan) was used as a substrate of HRP, and the signals were visualized with a ChemiDoc™ MP System (Bio-Rad, Hercules, CA), and quantified with ImageJ software.

Immunofluorescence microscopy. Immunofluorescence staining was performed according to the protocol described elsewhere with slight modification (Fujimoto et al., 2015; Hirota and Tanaka, 2009). Briefly, COS-1 cells were immobilized on coverslips with 4% paraformaldehyde in PBS (pH 7.4) for 30 minutes at room temperature, and sequentially quenched with 50 mM NH$_4$Cl in PBS for 15 minutes. Permeabilization and blocking was simultaneously conducted by treating the samples with PBS containing 0.05% saponin and 1% bovine serum albumin (BSA, fraction V) for 30 minutes. The cells were incubated with the following primary antibodies for 1 hr at room temperature; rabbit anti-CD4 antibody (H-370, Santa Cruz Biotechnology, Dallas, TX), rabbit anti-HA-tag antibody (Sigma Aldrich), rabbit anti-UGT2B7 antibody (Proteintech, Rosemont, IL), and mouse anti-CNX antibody (BD Biosciences) were diluted 300-fold with PBS containing 0.05% saponin and 1% BSA. After a PBS wash (5 minutes ×3), the cells were incubated for 30 minutes at room temperature with Alexa488- and Cy3-labeled secondary antibodies, together with 4',6-diamidino-2-phenylindole (DAPI) as a nuclear counterstain. The secondary antibody was diluted 300-fold with PBS containing 0.05% saponin and 1% BSA, and concentration of DAPI was 1 µg/mL in use. After a PBS wash (5 minutes ×3), coverslips were mounted in MOWIOL 4-88 (Merck Millipore) onto glass slides, and the samples were analyzed by the LSM 700 laser scanning confocal microscope (Carl Zeiss, Oberkochen,

9

Germany) equipped with four lasers (405, 455, 555, and 639 nm). The objective lens used in the analysis was Plan-Apochromat 63x/1.4 Oil DIC. To obtain multiple stained images, laser and filter were optimized automatically for each fluorescence label. Image files were created from low data with ZEISS Efficient Navigation (ZEN) software, and photographic images were processed using Photoshop (Adobe Systems, San Jose, CA). Colocalization of UGT2B7 and CNX were quantified with ZEN software.

Detection of aggregated forms of UGT2B7-HA and its mutants by Triton X-100 treatment. Triton X-100 soluble and insoluble fractions were prepared as described elsewhere with slight modifications (Hirota and Tanaka, 2009). In brief, COS-1 cells transiently expressing UGT2B7-HA and its mutants were harvested in cold sucrose solution (0.25 M sucrose, 1 mM EDTA, 10 mM Hepes, pH 7.4), homogenized by 25 passages through a 23 gauge needle connected to a 1 ml syringe, and subsequently centrifuged at 1,000rpm for 10 min. The resulting post-nuclear supernatants (homogenate) were centrifuged at 105000×g for 1 hr, and fractionated into membrane (pellet) and cytosol (supernatant). Membrane fractions were solubilized in 1% Triton X-100 in PBS, and divided into soluble (Sol.) and insoluble (ppt) fractions by centrifugation (105000×g, 4°C, 1 hr). Insoluble fractions were further solubilized in RIPA buffer, 50 mM Tris-HCl (pH 7.5) containing 150 mM NaCl, 1 mM EDTA, 1% NP-40, 0.1% SDS, and 0.05% sodium deoxycholate. Volumes of each fraction were kept equal, and then homogenate (15 μg protein) and equivalent volumes of the later fractions were analyzed by immunoblotting.

Treatments with proteasome and lysosome inhibitors. UGT2B7-HA, ΔCT-HA, and ΔTM-HA were transiently expressed in COS-1 cells. Twelve hr after transfection, the cells were treated with 1 μM proteasome inhibitor (MG132) and lysosome inhibitor cocktail, 10 μg/mL E-64d, 20 μg/mL leupeptin, and 10 μg/mL pepstatin A for 12 hr. Whole cell lysates were prepared, and analyzed by immunoblotting.

Secretion of the cytoplasmic and transmembrane domain-deleted mutants of UGT2B7 and CD4. COS-1 cells were transfected with each construct and cultured for 12 hr in 1 mL FBS-free DMEM. Cells were harvested in cold sucrose solution, and whole lysates were prepared as above mentioned. Medium were also collected and 400 μL of them were mixed with 100 uL of 50% trichloroacetic acid, and incubated on ice for 10 min. After centrifugation, precipitants were washed with ice-cold acetone twice, and analyzed by immunoblotting.

Other Methods. Protein concentrations of baculosomes were determined by the method of Lowry *et al.* (Lowry et al., 1951), and those of COS-1 cell lysates were by Protein Assay CBB Solution (Nacalai Tesque) with BSA as a standard.

Results

To assess the role of the C-terminal region of UGT2B7, including the di-lysine motif, in its ER localization, we designed a series of deletion mutants lacking the di-lysine motif (ΔDM), cytosolic tail (ΔCT), and transmembrane helix (ΔTM), respectively, as illustrated in Fig. 2A. Each deletion mutant, as well as UGT2B7 wild-type (WT), were expressed in Sf9 insect cells and their expression was analyzed by immunoblotting with goat anti-mouse low p*I* form UGT antibody (Mackenzie et al., 1984). Using this antibody, we observed a single band in cell lysates expressing each UGT2B7 construct, which had the predicted molecular weight based on the size of the deletion (Fig. 2B). To determine subcellular localization of the UGT2B7 mutants, we fractionated the homogenates prepared from insect cells simultaneously infected with recombinant baculovirus coding human CNX as an ER marker. We obtained three fractions, nuclei & mitochondria, microsomes, and cytosol for each sample. All of the deletion mutants were exclusively collected in the microsomal fraction, similar to CNX (Fig. 2C), in agreement with our last report (Miyauchi et al., 2015). To further investigate their subcellular localization, we conducted immunofluorescence staining to analyze co-localization of UGT2B7 and endogenous CNX in COS-1 cells. Overexpressed wild-type UGT2B7 showed a reticular staining pattern and co-localized with CNX (Fig. 3A top and middle panels). Unfortunately, the epitope of UGT2B7 recognized by the anti-UGT2B7 antibody is not clear. Accordingly, in later analyses using several deletion mutants, we added a HA-tag to the C-terminus in order to detect the mutants using an immunochemical approach. Before detection of the mutant with the anti-HA-tag antibody, we determined whether the HA-tag affects localization of UGT2B7 WT. As shown in Fig. 3A, both HA-tagged and non-tagged UGT2B7 WT were recognized equally by anti-UGT2B7 antibody, and addition of the HA-tag to the C-terminal end did not alter the staining pattern. Next, we conducted staining of the C-terminal deletion mutants with anti-HA-tag antibody. As shown in Fig. 3B, ΔDM, ΔCT, and ΔTM mutants co-localized with CNX, similar to WT-HA, indicating that about 80-95% of UGT2B7 WT/deletion mutants were colocalized with CNX (Fig. 3C). These results support the results of the fractionation approach (Fig. 2C). A chimeric protein that replaced the cytoplasmic domain of CD4 with that of UGT2B7 (CD4-UGT) also co-localized with CNX. However, it was redistributed to the cell surface by the substitution of two lysines with alanines within the cytoplasmic domain (CD4-UGT-2KA) (Figs. 3D and E), suggesting that the di-lysine motif acts as an ER retention signal in this chimera. Intriguingly, in contrast to the case of UGT2B7 (Fig. 3A), fusion of the HA-tag to the C-terminus of CD4-UGT (CD4-UGT-HA) altered the ER distribution of CD4-UGT to the cell surface (Figs. 3D and E), consistent with a previous report demonstrating that the proper positioning of two lysine residues from the carboxyl-terminus is critical for retention of ER resident membrane proteins (Jackson et al., 1990). Collectively, our data suggest that the di-lysine motif within the cytoplasmic domain of UGT2B7

is sufficient to localize CD4 to the ER but not necessary for the ER retention of UGT2B7.

The results described above led us to speculate that the luminal domain of UGT2B7 is required for ER retention. In addition, it has been reported that the 141-240 region of human UGT1A6 is another membrane-associated domain and functions as an ER retention signal (Ouzzine et al., 1999). When this region was transplanted to the cytoplasmic green fluorescent protein (EGFP), the UGT 141-240/EGFP chimera was localized to the ER. Based on these findings, we first focused on the N-terminal half domain of UGT2B7 (24-252; except signal peptide) to explore the region(s) necessary for ER retention. We generated five deletion mutants (Δ1-HA to Δ5-HA) systematically lacking 30 residue sections containing two or three predicted helices from the C-terminal end of UGT2B7 (24-252), and a HA-tag was added to the C-terminal end of each deletion mutant (Fig. 4A). We transiently expressed these UGT2B7 mutants in Sf9 insect cells and confirmed their expression by immunoblotting (Fig. 4B). We further performed subcellular fractionation of insect cells expressing these deletion mutants using the same procedure, as in Fig. 2C. The results showed that all of the mutants were exclusively detected in the microsomal fraction with coexpressed CNX (Fig. 4C). Moreover, consistent with the results of subcellular fractionation, the results of immunofluorescence microscopy in COS-1 cells also showed that all of the deletion mutants colocalized with CNX in reticular-like structures (Fig. 5A) and 90% of these mutants colocalized with CNX (Fig. 5B). Taken together, these results suggest that at least the N-terminal 24-133 region may be necessary for retention of UGT2B7 in the ER.

To verify the necessity of the 24-133 residue region for ER retention of UGT2B7, we created a deletion mutant of this domain (Δ6-HA) and analyzed its expression and localization in COS-1 cells (Figs. 6A-C). To our surprise, UGT2B7 Δ6-HA localized to CNX-positive reticular-like structures. We further generated a series of deletion mutants of the UGT2B7 luminal domain (Fig. 6A). These deletion mutants were transiently expressed in COS-1 cells and their expression and localization analyzed using immunoblotting and immunofluorescence microscopy, respectively (Figs. 6B and C). As shown in Fig. 6C, despite the systematic truncation, all of the mutants were observed in the reticular-like structures and co-localized with CNX. Moreover, 80-95% of the serial mutants colocalized with CNX (Fig. 6D) as same as UGT2B7 WT (Fig. 3C). Collectively, these data imply that UGT2B7 could localize in the ER without any signal sequence rather than the presence of a possible signal for the retention to the ER. Moreover, it is well known that proteins which aggregate in cells are largely detergent insoluble (Hirota and Tanaka, 2009; Imai et al., 2001). When we solubilized microsomes expressing these deletion mutants with 1% Triton X-100, they were predominantly recovered in solubilized fractions (Fig. 7A), indicating that they were properly folded, and thereby ruling out the possibility that the ER localization of these mutants resulted from accumulation in the ER by unfolding or misfolding. Moreover, we examined stability of UGT2B7-HA deletion mutants (ΔCT and ΔTM) using inhibitors of

proteasome and lysosomal degradation. Treatment with MG132, a proteasome inhibitor, but not with lysosomal protease inhibitors, increased protein levels of WT, ΔCT and ΔTM of UGT2B7 (Figs. 7B and C), thereby suggesting that deletion of both the cytoplasmic and transmembrane domains did not affect the stability of mutant proteins.

Deletions of the transmembrane domain of membrane proteins transported by the secretary pathway should result in their secretion into the medium, unless they contain a retention signal in the remaining domain (Paabo et al., 1987; Paabo et al., 1986). We examined whether both cytoplasmic and transmembrane domain-deleted mutants of UGT2B7 and CD4 were secreted. Although all of the deletion mutants of UGT2B7-HA (ΔTM, Δ1, and Δ7) were detected only in cell lysates, CD4-ΔTM was significantly secreted into the cultured medium (Fig. 7D).

Discussion

The di-lysine motif is one representative peptide for motif-based retrograde transportation, but it is controversial whether this motif is indeed necessary for ER localization of UGTs. In this study, we present evidence that C-terminal deletion mutants of UGT2B7 including ΔDM, ΔCT, and ΔTM can localize to the ER in their folded states (Figs. 2C, 3B, 3C, and 7). It has been demonstrated previously that the proper positioning of two lysines at -3 and -4 or -5 from the carboxyl-terminus is critical for retention of ER resident membrane proteins, because addition or deletion of residues from the C-terminus decreased retention efficiency (Jackson et al., 1990). Indeed, we also confirmed this finding, using the chimeric protein, CD4-UGT (Fig. 3D). However, our findings that not only UGT2B7ΔDM, but also UGT2B7-HA, in which the positions of two lysine residues were shifted from -3 and -5 to -12 and -14 by adding a HA-tag to the C-terminus, localized to the ER (Fig. 3B) suggest that the C-terminal di-lysine motif of UGT2B7 is unnecessary for its ER localization, supporting previous reports (Meech and Mackenzie, 1997; Meech et al., 1996; Ouzzine et al., 1999). Of note, there are ER-located splice variants of human UGT, which lack the transmembrane and cytoplasmic domains (Bellemare et al., 2010; Girard et al., 2007; Guillemette et al., 2014; Levesque et al., 2007; Rouleau et al., 2014). Similar variants of UGT2B7 showed ER localization despite lacking the di-lysine motif (Menard et al., 2013). These findings also reinforce our conclusion that the cytoplasmic region including the di-lysine motif is not required for ER retention.

In contrast, previous studies have brought attention to the role of the di-lysine motif as a retrieval signal for UGT. Transplantation of the motif altered subcellular localizations of some plasma membrane proteins to the ER (Jackson et al., 1990; Kinosaki et al., 1993). Moreover, it was reported that the interaction of rat UGT2B1 with β-COP, a subunit in the COPI complex, was abolished by deletion of the C-terminal cytoplasmic tail of UGT2B1 (Meech and Mackenzie, 1998). Given that UGT2B7 is statically retained in the ER, what is the physiological role of the C-terminal region containing the di-lysine motif? One possibility is to retrieve UGT2B7 that has escaped to post-ER compartments via non-specific transport known as "bulk flow". Details for the transport of proteins from the ER by bulk flow remain unclear (Barlowe and Helenius, 2016). Retrieval mediated by the di-lysine motif should return UGT2B7 to the ER against such a leak mechanism. The importance of this region on catalytic activity was also reported with another UGT isoform. The activity of a water-soluble UGT1A9 mutant lacking the transmembrane and cytoplasmic domains (UGT1A9sol), which was purified from an insect cell-expression system, was one order of magnitude lower than microsomal wild-type UGT1A9 (Kurkela et al., 2004). In addition, we have reported previously that the C-terminal region of UGT2B7 is important for its functional interaction with CYP3A4 (Miyauchi et al., 2015). UGT2B7 wild-type significantly suppressed CYP3A4 activity, but this suppression disappeared with ΔCT and ΔTM. These lines

of evidence clearly indicate a novel role for the UGT C-terminal region as a domain regulating UGT activity and the activity of other drug metabolizing enzymes, which may improve our understanding of the large inter-individual differences in *in vivo* catalytic activity of UGT and P450 (Court, 2010; Lamba et al., 2002; Shimada et al., 1994).

ER controls quality of the synthesized proteins, and unfolded and misfolded ones are degraded by endoplasmic reticulum-associated degradation (ERAD) (Nakatsukasa and Brodsky, 2008). In this study, we showed that all UGT mutants were predominantly collected in the soluble fraction, thereby suggesting that they were folded correctly (Fig. 7A). Moreover, there was no difference in protein stability among wild-type and the mutants. These results demonstrated that the ER localization of the mutants is not due to protein misfolding.

Serial mutation analyses suggest that retention or retrieval signals are not needed for ER localization of UGT2B7 in this study. Although many ER membrane proteins do not bear a di-lysine motif in their C-terminal ends, they are positioned in the ER, indicating the presence of another mechanism underlying ER localization of membrane protein (Teasdale and Jackson, 1996). One of postulated mechanism is that the proteins should have a novel retrieval/retention signal. Previous studies have suggested the presence of ER retention signals of UGT isoforms in either the luminal domain or the cytoplasmic and transmembrane domains (Table 1). However, all of the UGT2B7 deletion mutants we have constructed were observed in the ER without being secreted (Fig. 7D). Thus, it seems more reasonable to assume that UGT2B7 lacks an active signal required for exit from the ER, which results in passive and static retention in the ER (Fig. 8), although little is known about such an export signal.

Further studies are necessary to clarify the molecular mechanism underlying UGT localization in the ER, which may improve our understanding of how ER membrane proteins reside in their respective membrane compartments without retention and/or retrieval motifs.

Acknowledgements

Conflict of Interest

The authors declare that the research was conducted in the absence of any commercial or financial relationships that could be construed as a potential conflict of interest.

Authorship Contribution

Participated in research design: Miyauchi, Kimura S., Kimura A., Kurohara, Hirota, Fujimoto, Mackenzie, Tanaka, Ishii

Conducted experiments: Miyauchi, Kimura S., Kimura A., Kurohara, Hirota

Performed data analysis: Miyauchi, Kimura S., Kimura A., Kurohara, Hirota, Fujimoto

Wrote or contributed the writing of the manuscript: Miyauchi, Mackenzie, Tanaka, Ishii

References

Barlowe C and Helenius A (2016) Cargo Capture and Bulk Flow in the Early Secretory Pathway. *Annu Rev Cell Dev Biol* **32**: 197-222.

Barre L, Magdalou J, Netter P, Fournel-Gigleux S and Ouzzine M (2005) The stop transfer sequence of the human UDP-glucuronosyltransferase 1A determines localization to the endoplasmic reticulum by both static retention and retrieval mechanisms. *FEBS J* **272**: 1063-1071.

Bellemare J, Rouleau M, Harvey M and Guillemette C (2010) Modulation of the human glucuronosyltransferase UGT1A pathway by splice isoform polypeptides is mediated through protein-protein interactions. *J Biol Chem* **285**: 3600-3607.

Bock KW (2012) Human UDP-glucuronosyltransferases: feedback loops between substrates and ligands of their transcription factors. *Biochem Pharmacol* **84**: 1000-1006.

Bowalgaha K, Elliot DJ, Mackenzie PI, Knights KM and Miners JO (2007) The glucuronidation of Δ4-3-Keto C19- and C21-hydroxysteroids by human liver microsomal and recombinant UDP-glucuronosyltransferases (UGTs): 6α- and 21-hydroxyprogesterone are selective substrates for UGT2B7. *Drug Metab Dispos* **35**: 363-370.

Chowdhury JR, Novikoff PM, Chowdhury NR and Novikoff AB (1985) Distribution of UDPglucuronosyltransferase in rat tissue. *Proc Natl Acad Sci U S A* **82**: 2990-2994.

Court MH (2010) Interindividual variability in hepatic drug glucuronidation: studies into the role of age, sex, enzyme inducers, and genetic polymorphism using the human liver bank as a model system. *Drug Metab Rev* **42**: 209-224.

Evans WE and Relling MV (1999) Pharmacogenomics: translating functional genomics into rational therapeutics. *Science* **286**: 487-491.

Fujimoto K, Ida H, Hirota Y, Ishigai M, Amano J and Tanaka Y (2015) Intracellular Dynamics and Fate of a Humanized Anti-Interleukin-6 Receptor Monoclonal Antibody, Tocilizumab. *Mol Pharmacol* **88**: 660-675.

Gaynor EC, te Heesen S, Graham TR, Aebi M and Emr SD (1994) Signal-mediated retrieval of a membrane protein from the Golgi to the ER in yeast. *J Cell Biol* **127**: 653-665.

Girard H, Levesque E, Bellemare J, Journault K, Caillier B and Guillemette C (2007) Genetic diversity at the UGT1 locus is amplified by a novel 3' alternative splicing mechanism leading to nine additional UGT1A proteins that act as regulators of glucuronidation activity. *Pharmacogenet Genomics* **17**: 1077-1089.

Gomez-Navarro N and Miller E (2016) Protein sorting at the ER-Golgi interface. *J Cell Biol* **215**: 769-778.

Guillemette C, Levesque E and Rouleau M (2014) Pharmacogenomics of human uridine diphospho-glucuronosyltransferases and clinical implications. *Clin Pharmacol Ther* **96**: 324-339.

Harding D, Wilson SM, Jackson MR, Burchell B, Green MD and Tephly TR (1987) Nucleotide and deduced

amino acid sequence of rat liver 17 beta-hydroxysteroid UDP-glucuronosyltransferase. *Nucleic Acids Res* **15**: 3936.

Hirota Y and Tanaka Y (2009) A small GTPase, human Rab32, is required for the formation of autophagic vacuoles under basal conditions. *Cell Mol Life Sci* **66**: 2913-2932.

Imai Y, Soda M, Inoue H, Hattori N, Mizuno Y and Takahashi R (2001) An unfolded putative transmembrane polypeptide, which can lead to endoplasmic reticulum stress, is a substrate of Parkin. *Cell* **105**: 891-902.

Ishii Y, Koba H, Kinoshita K, Oizaki T, Iwamoto Y, Takeda S, Miyauchi Y, Nishimura Y, Egoshi N, Taura F, Morimoto S, Ikushiro S, Nagata K, Yamazoe Y, Mackenzie PI and Yamada H (2014) Alteration of the function of the UDP-glucuronosyltransferase 1A subfamily by cytochrome P450 3A4: different susceptibility for UGT isoforms and UGT1A1/7 variants. *Drug Metab Dispos* **42**: 229-238.

Iyanagi T, Haniu M, Sogawa K, Fujii-Kuriyama Y, Watanabe S, Shively JE and Anan KF (1986) Cloning and characterization of cDNA encoding 3-methylcholanthrene inducible rat mRNA for UDP-glucuronosyltransferase. *J Biol Chem* **261**: 15607-15614.

Jackson MR, Nilsson T and Peterson PA (1990) Identification of a consensus motif for retention of transmembrane proteins in the endoplasmic reticulum. *EMBO J* **9**: 3153-3162.

Jackson MR, Nilsson T and Peterson PA (1993) Retrieval of transmembrane proteins to the endoplasmic reticulum. *J Cell Biol* **121**: 317-333.

Kinosaki M, Masuko T, Sogawa K, Iyanagi T, Yamamoto T, Hashimoto Y and Fujii-Kuriyama Y (1993) Intracellular localization of UDP-glucuronosyltransferase expressed from the transfected cDNA in cultured cells. *Cell Struct Funct* **18**: 41-51.

Kurkela M, Morsky S, Hirvonen J, Kostiainen R and Finel M (2004) An active and water-soluble truncation mutant of the human UDP-glucuronosyltransferase 1A9. *Mol Pharmacol* **65**: 826-831.

Lamba JK, Lin YS, Schuetz EG and Thummel KE (2002) Genetic contribution to variable human CYP3A-mediated metabolism. *Adv Drug Deliv Rev* **54**: 1271-1294.

Levesque E, Girard H, Journault K, Lepine J and Guillemette C (2007) Regulation of the UGT1A1 bilirubin-conjugating pathway: role of a new splicing event at the UGT1A locus. *Hepatology* **45**: 128-138.

Lowry OH, Rosebrough NJ, Farr AL and Randall RJ (1951) Protein measurement with the Folin phenol reagent. *J Biol Chem* **193**: 265-275.

Mackenzie PI, Hjelmeland LM and Owens IS (1984) Purification and immunochemical characterization of a low-pI form of UDP glucuronosyltransferase from mouse liver. *Arch Biochem Biophys* **231**: 487-497.

Meech R and Mackenzie PI (1997) Structure and function of uridine diphosphate glucuronosyltransferases. *Clin Exp Pharmacol Physiol* **24**: 907-915.

Meech R and Mackenzie PI (1998) Determinants of UDP glucuronosyltransferase membrane association and residency in the endoplasmic reticulum. *Arch Biochem Biophys* **356**: 77-85.

Meech R, Yogalingam G and Mackenzie PI (1996) Mutational analysis of the carboxy-terminal region of UDP-glucuronosyltransferase 2B1. *DNA Cell Biol* **15**: 489-494.

Menard V, Collin P, Margaillan G and Guillemette C (2013) Modulation of the UGT2B7 enzyme activity by C-terminally truncated proteins derived from alternative splicing. *Drug Metab Dispos* **41**: 2197-2205.

Miyauchi Y, Nagata K, Yamazoe Y, Mackenzie PI, Yamada H and Ishii Y (2015) Suppression of Cytochrome P450 3A4 Function by UDP-Glucuronosyltransferase 2B7 through a Protein-Protein Interaction: Cooperative Roles of the Cytosolic Carboxyl-Terminal Domain and the Luminal Anchoring Region. *Mol Pharmacol* **88**: 800-812.

Munro S and Pelham HR (1987) A C-terminal signal prevents secretion of luminal ER proteins. *Cell* **48**: 899-907.

Nakatsukasa K and Brodsky JL (2008) The recognition and retrotranslocation of misfolded proteins from the endoplasmic reticulum. *Traffic* **9**: 861-870.

Nilsson T, Jackson M and Peterson PA (1989) Short cytoplasmic sequences serve as retention signals for transmembrane proteins in the endoplasmic reticulum. *Cell* **58**: 707-718.

Ouzzine M, Barre L, Netter P, Magdalou J and Fournel-Gigleux S (2006) Role of the carboxyl terminal stop transfer sequence of UGT1A6 membrane protein in ER targeting and translocation of upstream lumenal domain. *FEBS Lett* **580**: 1953-1958.

Ouzzine M, Magdalou J, Burchell B and Fournel-Gigleux S (1999) An internal signal sequence mediates the targeting and retention of the human UDP-glucuronosyltransferase 1A6 to the endoplasmic reticulum. *J Biol Chem* **274**: 31401-31409.

Paabo S, Bhat BM, Wold WS and Peterson PA (1987) A short sequence in the COOH-terminus makes an adenovirus membrane glycoprotein a resident of the endoplasmic reticulum. *Cell* **50**: 311-317.

Paabo S, Weber F, Nilsson T, Schaffner W and Peterson PA (1986) Structural and functional dissection of an MHC class I antigen-binding adenovirus glycoprotein. *EMBO J* **5**: 1921-1927.

Pelham HR (1988) Evidence that luminal ER proteins are sorted from secreted proteins in a post-ER compartment. *EMBO J* **7**: 913-918.

Radominska-Pandya A, Czernik PJ, Little JM, Battaglia E and Mackenzie PI (1999) Structural and functional studies of UDP-glucuronosyltransferases. *Drug Metab Rev* **31**: 817-899.

Radominska-Pandya A, Ouzzine M, Fournel-Gigleux S and Magdalou J (2005) Structure of UDP-glucuronosyltransferases in membranes. *Methods Enzymol* **400**: 116-147.

Rouleau M, Roberge J, Bellemare J and Guillemette C (2014) Dual roles for splice variants of the glucuronidation pathway as regulators of cellular metabolism. *Mol Pharmacol* **85**: 29-36.

Rowland A, Miners JO and Mackenzie PI (2013) The UDP-glucuronosyltransferases: their role in drug

metabolism and detoxification. *Int J Biochem Cell Biol* **45**: 1121-1132.

Schrader M, Godinho LF, Costello JL and Islinger M (2015) The different facets of organelle interplay-an overview of organelle interactions. *Front Cell Dev Biol* **3**: 56.

Shepherd SR, Baird SJ, Hallinan T and Burchell B (1989) An investigation of the transverse topology of bilirubin UDP-glucuronosyltransferase in rat hepatic endoplasmic reticulum. *Biochem J* **259**: 617-620.

Shim SH (2017) Cell imaging: An intracellular dance visualized. *Nature* **546**: 39-40.

Shimada T, Yamazaki H, Mimura M, Inui Y and Guengerich FP (1994) Interindividual variations in human liver cytochrome P-450 enzymes involved in the oxidation of drugs, carcinogens and toxic chemicals: studies with liver microsomes of 30 Japanese and 30 Caucasians. *J Pharmacol Exp Ther* **270**: 414-423.

Teasdale RD and Jackson MR (1996) Signal-mediated sorting of membrane proteins between the endoplasmic reticulum and the golgi apparatus. *Annu Rev Cell Dev Biol* **12**: 27-54.

Ziegler K, Tumova S, Kerimi A and Williamson G (2015) Cellular asymmetric catalysis by UDP-glucuronosyltransferase 1A8 shows functional localization to the basolateral plasma membrane. *J Biol Chem* **290**: 7622-7633.

Footnotes

Presented in part at:

28th Japanese Society of the Study of Xenobiotics (JSSX) (2013), 134th Annual meeting of Japanese Society of Pharmaceutical Sciences (2014), Joint meeting of 19th North American Regional Meeting of International Society for the Study of Xenobiotics (ISSX)-29th JSSX (2014) (Kimura S. et al); Forum 2017: Pharmaceutical Health Care and Environmental Toxicology (2017) (Miyauchi et al)

Figure Legends

Fig. 1. Postulated topology of UGT2B7 in the endoplasmic reticulum membrane

Fig. 2. Subcellular localization of Sf9 cells infected with cytoplasmic tail- and/or transmembrane domain-deletion mutants of UGT2B7. (A) Schematic sequences of UGT2B7 deletion mutants. The numbers represent the residue position of wild-type UGT2B7 counted from the N-terminus. SP, signal peptide; DM, di-lysine motif; CT, cytosolic tail; TM, transmembrane region (B) Immunoblotting to confirm expression of wild-type UGT2B7 and its mutants in insect cells. Sf9 cells, transfected with recombinant bacmids to obtain P1 viruses, were lysed and analyzed. After collection of P1 viruses, the pelleted cells were re-suspended in PBS, and an aliquot of the suspension was mixed with 2×SDS-PAGE sample buffer to prepare whole cell lysates. HLM and Mock represent human liver microsomes (5 μg protein) and baculosomes prepared from Sf9 cells infected with control viruses (10 μg), respectively. Anti-mouse UGT antibody was used as a primary antibody (Mackenzie et al., 1984). (C) Fractionations of Sf9 cells to determine localization of the UGT2B7 mutants. UGT2B7 wild-type/mutants were simultaneously overexpressed with calnexin (CNX) in Sf9 cells. Sf9 homogenates were fractionated by sequential centrifugation. The fractions were analyzed by immunoblotting to determine the UGT2B7 wild-type/mutant subcellular localization. Protein amounts of loaded fractions are indicated below: homogenate (Homo), 10 μg; nuclei, 2 μg; mitochondria (MT), 2.5 μg; microsomes (MS), 5 μg; cytosol (Cyt), 7 μg. Anti-mouse UGT antibody and anti-CNX antibody were utilized as primary antibodies. Each band was quantified with ImageJ software, and was shown as % of total.

Fig. 3. Localization of the cytoplasmic tail and/or transmembrane domain-deleted mutants of UGT2B7 and the CD4-UGT chimeric protein in COS-1 cells. COS-1 cells transfected with UGT2B7 wild-type (WT) or the mutants were fixed and stained 24 hr after transfection. (A) Localization of UGT2B7 and UGT2B7-HA (UGT2B7 with a C-terminal HA-tag) were compared with anti-UGT2B7 antibody (green). Cells were also stained red with an antibody to endogenous calnexin (CNX), a marker protein of the endoplasmic reticulum. In the merged panels, nuclei stained by DAPI are shown in cyan. (B) Localization of the C-terminal deleted mutants of UGT2B7. The sequences of the mutants are shown in Fig. 2A. A HA-tag was conjugated to their C-terminus for immunochemical detection. Cells were stained with anti-HA antibody (green) and anti-CNX (red). (C) Colocalization of UGT2B7 WT/mutants and CNX were quantified, and the mean ± S.D. values are shown. (D) Schematic sequences of CD4 and its chimeric proteins whose cytoplasmic domains were replaced with that of UGT2B7. The numbers represent the residue position of wild-type CD4 counted from the N-terminus. The di-lysine motif of UGT2B7 is highlighted in the C-terminus of each chimera. SP, signal peptide; CT, cytosolic tail; TM,

transmembrane region (E) Localization of CD4 chimeric proteins. CD4-UGT represents a CD4 chimera whose cytoplasmic domain was replaced with that of UGT2B7. Cells were stained with anti-CD4 antibody which recognizes the extracellular domain of CD4 (green) and anti-CNX (red). In merged panels, the nuclei are shown in cyan, and each scale bar represents 10 μm.

Fig. 4. Subcellular localization of a series of C-terminal truncated mutants of UGT2B7 in Sf9 infected cells. (A) Schematic sequences of C-terminal truncated UGT2B7 mutants. The numbers represent the residue position of wild-type UGT2B7 (WT) counted from the N-terminus. A hemagglutinin epitope tag was conjugated to the C-terminus for detection by immunochemical methods. SP, signal peptide; TM, transmembrane region; DM, di-lysine motif; HA, Hemagglutinin (B) Immunoblotting to detect UGT2B7 mutants in insect cells. Sf9 cells transfected with recombinant bacmids to obtain P1 viruses were lysed and analyzed. After collection of P1 viruses, the pelleted cells were re-suspended in PBS, and an aliquot of the suspension was mixed with 2×SDS-PAGE sample buffer to prepare whole cell lysates. WT-HA and Mock represent UGT2B7-HA microsomes (5 μg) and control microsomes (10 μg), respectively. Anti-HA-tag antibody was used as a primary antibody. (C) Fractionations of Sf9 cells to determine localization of the UGT2B7 mutants. Human CNX was also transfected in cells expressing UGT2B7 deletion mutants. Sf9 homogenates were fractionated by sequential centrifugation. Protein amounts of loaded fractions were: homogenate (Homo), 15 μg; nuclei, 6 μg; mitochondria (MT), 6 μg; microsomes (MS), 5 μg; cytosol (Cyt), 10 μg. Anti-HA antibody and Anti-CNX antibody were used as primary antibodies. Each band was quantified with ImageJ software, and was shown as % of total.

Fig. 5. (A) Localization of C-terminal-truncated mutants of UGT2B7 in transfected COS-1 cells. Schematic sequences of the mutants are presented in Fig. 4A. All of the mutants were fused with a HA-tag at their C-termini for immunochemical detection. COS-1 cells transiently expressing the mutants were stained with anti-HA antibody (green). Endogenous CNX was also visualized with anti-CNX antibody (red) as an ER marker. Nuclei stained with DAPI are shown in cyan, and each scale bar represents 10 μm in the merge panels. (B) Colocalization of UGT2B7 mutants and CNX were quantified, and the mean ± S.D. values are shown.

Fig. 6. Localization of internal deletion mutants of UGT2B7 in transfected COS-1 cells. (A) Schematic sequences of UGT2B7 mutants (Δ6-HA to Δ11-HA). (B) Immunoblotting to detect the UGT2B7 mutants in COS-1 cells. Cells were transfected with 2 μg vector coding each UGT2B7 mutant, and lysed 24 hr after transfection. The lysates (20 μg) were analyzed by immunoblotting. Anti-HA antibody was used as a primary antibody. (C) Immunofluorescence to show co-

localizations of the UGT2B7 mutants with CNX. The mutants were transiently expressed in COS-1 cells, and visualized with anti-HA antibody (green). Endogenous CNX was also stained with anti-CNX antibody (red) as an ER marker. Nuclei were stained with DAPI and are shown in cyan, and each scale bar represents 10 μm in the merge panel. (D) Colocalization of UGT2B7 mutants and CNX were quantified, and the mean ± S.D. values are shown.

Fig. 7. Analysis of stability and secretion of the UGT2B7-HA mutants. (A) Triton X-100 treatment of microsomal fractions to detect aggregated forms of UGT2B7-HA and its mutants. Homogenates (Homo) were prepared from COS-1 cells with a syringe equipped with a 23 gauge needle followed by low-speed centrifugation. An aliquot of homogenate was further fractionated by ultracentrifugation, and supernatants and pellets were collected as cytosols (Cyt) and microsomes, respectively. Microsomes were solubilized in 1% Triton X-100, and separated into soluble fraction (Sol.) and insoluble pellet (ppt) by another ultracentrifugation. Homogenate (15 μg) and equivalent volumes of the later fractions were analyzed by immunoblotting. Upper and lower panels show the results in short and long exposures, respectively. (B) Effect of treatment with proteasome inhibitor (MG132) and lysosome inhibitor cocktail on expression levels of UGT2B7-HAs. COS-1 cells transfected with UGT2B7-HA and its deletion mutants (ΔCT and ΔTM) were treated with 1 μM MG132 or lysosome inhibitor cocktail, 10 μg/mL E-64d, 20 μg/mL leupeptin, and 10 μg/mL pepstatin A, for 12 hr. Whole cell lysates were prepared and 20 μg were analyzed in immunoblotting. (C) The experiments with the inhibitors were performed and quantified three times. Each bar represents mean ± S.D. of relative intensities as each control = 100%. (D) Secretion of UGT2B7-HA, CD4, and their deletion mutants were analyzed. COS-1 cells were transfected with each construct and cultured in FBS-free medium for 12 hr. Cells were harvested for lysate preparation, and medium were concentrated with TCA. The samples were analyzed by immunoblotting with anti-HA antibody and anti-CD4 as primary antibodies.

Fig. 8. Predicted mechanism underlying static retention of UGT2B7 in the ER. Lack of an export signal functions as a retention system excluding UGT2B7 from anterograde transport.
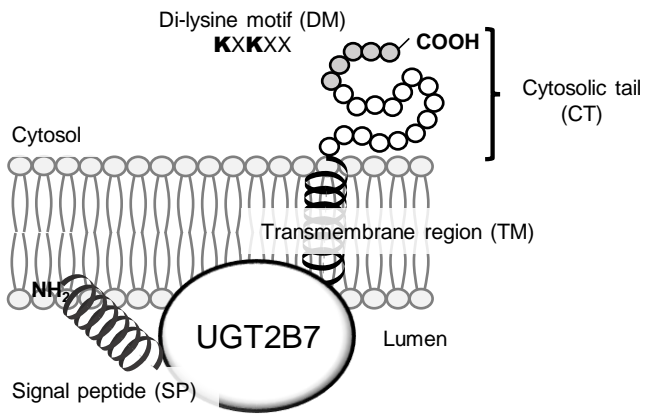
Table 1   The ER retention sites predicted for UGT isoforms

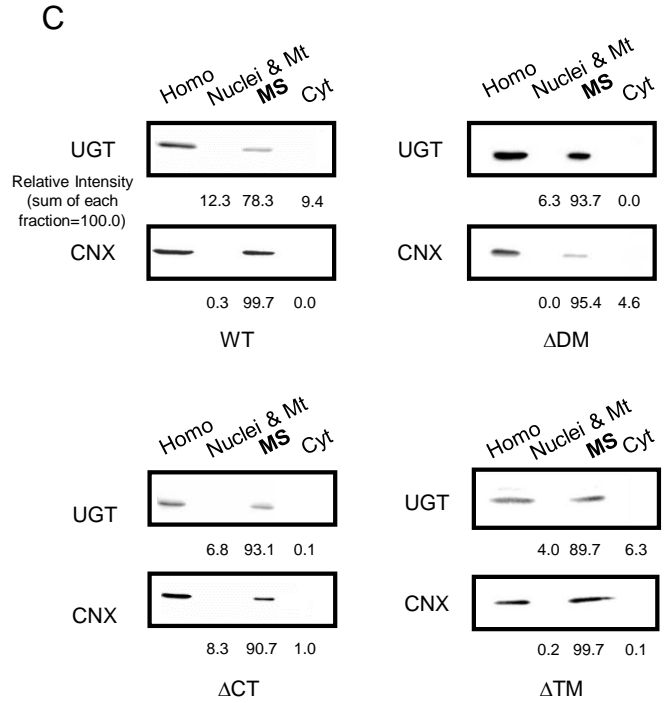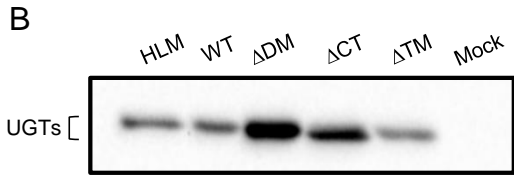| Isoform	Motif/Predicted position	Evidence	References
UGT common	Di-lysine motif	Nucleotide sequence Fusion protein with CD4/8 Fusion protein with ErbB2 **Fusion protein with CD4**	Iyanagi et al., 1986 Jackson et al., 1990; Kinosaki et al., 1993 **This study**
UGT2B1	Within 24-493	Truncated mutant	Meech et al., 1996
UGT1A6	Within 141-240	Fusion protein with GFP	Ouzzine et al., 1999
UGT1A(6)	490-506 (TMD)	Fusion proteins with CD4 Deletion mutants	Barre et al., 2005 Ouzzine et al., 2006
UGT1A(1)	Within 26-434	Splice variant i2	Bellemare et al., 2010 Girard et al., 2007 Guillemette et al., 2014 Levesque et al., 2007 Rouleau et al., 2014
UGT2B7	Within 24-369	Splice variant i4	Menard et al., 2013
UGT2B7	Within 24-492	Truncated mutant	Miyauchi et al., 2015
UGT2B7	**24-492 (ΔTM)** **24-252 (Δ1)** **24-133 (Δ5)** **253-492 (Δ7)** **471-492 (Δ8-Δ11)** **No obvious retention signal can be specified (Lack of a putative export signal)**	**Serial deletion mutants**	**This study**

TMD, transmembrane domain

Miyauchi et al   Figure 1

Miyauchi et al   Figure 2

A

WT

23   492 510   529

SP   TM   DM
⎰⎱
CT

ΔDM
(Δ525-529)

524

ΔCT
(Δ511-529)

510

ΔTM
(Δ493-529)

492

B

HLM WT ΔDM ΔCT ΔTM Mock

UGTs [

C

Homo Nuclei & Mt MS Cyt

UGT

Relative Intensity
(sum of each
fraction=100.0)   12.3 78.3   9.4

CNX

0.3 99.7   0.0

WT

Homo Nuclei & Mt MS Cyt

UGT

6.3 93.7   0.0

CNX

0.0 95.4   4.6

ΔDM

Homo Nuclei & Mt MS Cyt

UGT

6.8 93.1   0.1

CNX

8.3 90.7   1.0

ΔCT

Homo Nuclei & Mt MS Cyt

UGT

4.0 89.7   6.3

CNX

0.2 99.7   0.1

ΔTM

A

	UGT2B7	CNX	Merge
Mock			
WT			
WT-HA			

B

	HA	CNX	Merge
Mock			
WT-HA			
ΔDM-HA (Δ525-529)			
ΔCT-HA (Δ511-529)			
ΔTM-HA (Δ493-529)			

C

Colocalization ratio (ratio of UGT2B7s merged with CNX)

WT-HA   ΔDM-HA   ΔCT-HA   ΔTM-HA

D

CD4
25   397 418   458
SP   TM   CT

CD4-UGT
25   397 418
KG**K**ND
CT of UGT2B7
(510-529 of UGT2B7)

CD4-UGT-2KA
25   397 418
AGA**N**D
TM

CD4-UGT-HA
25   397 418
KG**K**ND
TM

: HA-tag

E

	CD4	CNX	Merge
Mock			
CD4			
CD4-UGT			
CD4-UGT-2KA			
CD4-UGT-HA			

Miyauchi et al   Figure 4

A

WT-HA

23   492 510   529

SP   TM   DM

Δ1-HA
(Δ253-529)

252

Δ2-HA
(Δ229-529)

228

Δ3-HA
(Δ204-529)

203

Δ4-HA
(Δ167-529)

166

Δ5-HA
(Δ134-529)

133

: HA-tag

B

(kDa)

WT-HA Δ1-HA Δ2-HA Δ3-HA Δ4-HA Δ5-HA Mock

60

45

35

25
20
15

C

Homo   Nuclei & Mt   MS   Cyt

HA
(UGT)
Relative Intensity
(sum of each
fraction=100.0)

0.4   97.9   1.7

CNX

7.8   91.2   1.0

Δ1-HA

Homo   Nuclei & Mt   MS   Cyt

HA
(UGT)

2.9   95.0   2.1

CNX

1.2   98.7   0.1

Δ2-HA

Homo   Nuclei & Mt   MS   Cyt

HA
(UGT)

3.1   96.7   0.2

CNX

1.4   98.4   0.2

Δ3-HA

Homo   Nuclei & Mt   MS   Cyt

HA
(UGT)

1.6   98.4   0.0

CNX

0.1   99.5   0.4

Δ4-HA

Homo   Nuclei & Mt   MS   Cyt

HA
(UGT)

0.2   99.7   0.1

CNX

0.6   99.3   0.1

Δ5-HA

A

| HA | CNX | Merge |

Δ1-HA
(Δ253-529

Δ2-HA
(Δ229-529

Δ3-HA
(Δ204-529)

Δ4-HA
(Δ167-529)

Δ5-HA
(Δ134-529)

B

Miyauchi et al   Figure 6

A

WT-HA
23   492 510   529
SP   TM   DM
CT

Δ6-HA
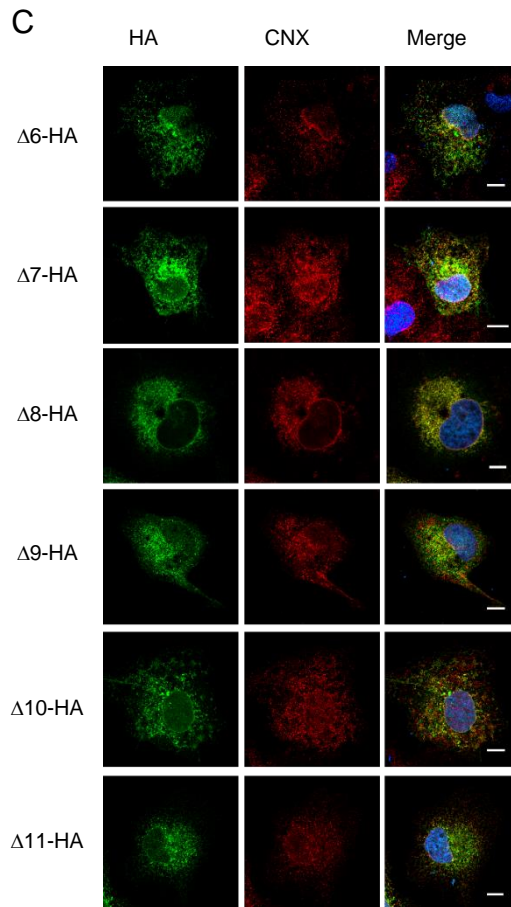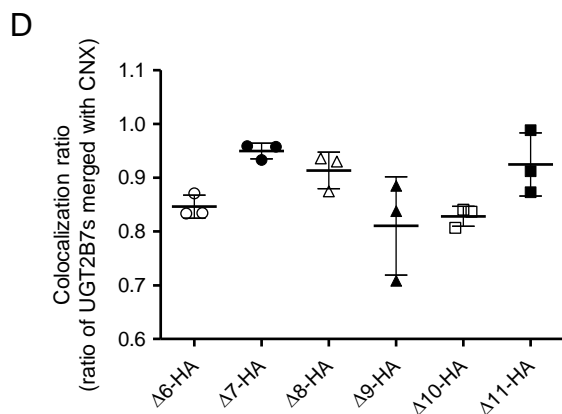(Δ24-133/TM)
134   492

Δ7-HA
(Δ24-252/TM)
253   492

Δ8-HA
(Δ24-310/TM)
311   492

Δ9-HA
(Δ24-252/311-367/TM)
310   368   492

Δ10-HA
(Δ24-252/368-421/TM)
367   422   492

Δ11-HA
(Δ24-252/422-470/TM)
421   471

B

(kDa)   Mock WT-HA Δ6-HA Δ7-HA Δ8-HA Δ9-HA Δ10-HA Δ11-HA
60
45
35
25
20
15

C

HA   CNX   Merge

Δ6-HA

Δ7-HA

Δ8-HA

Δ9-HA

Δ10-HA

Δ11-HA

D

Colocalization ratio
(ratio of UGT2B7s merged with CNX)

1.1
1.0
0.9
0.8
0.7
0.6

Δ6-HA Δ7-HA Δ8-HA Δ9-HA Δ10-HA Δ11-HA

A

Vector	WT-HA	ΔDM-HA	ΔCT-HA	ΔTM-HA	Δ7-HA
Fractions	**Homo** Cyt Sol. ppt	**Homo** Cyt Sol. ppt	**Homo** Cyt Sol. ppt	**Homo** Cyt Sol. ppt	**Homo** Cyt Sol. ppt

Anti-HA
(Short exposure)

70k
60k
45k
35k
25k

Anti-HA
(Long exposure)

70k
60k
45k
35k
25k

B

	WT-HA	ΔCT-HA	ΔTM-HA
	Control MG132 LIs	Control MG132 LIs	Control MG132 LIs

Anti-HA

Anti-β-actin

C

Relative expression
(Control=100%)

500
400
300
200
100
0

Control MG132 LIs | Control MG132 LIs | Control MG132 LIs
WT-HA | ΔCT-HA | ΔTM-HA

D

	Cell Lysate	Secretion
(kDa)	Mock WT-HA ΔTM-HA Δ1-HA Δ7-HA	Mock WT-HA ΔTM-HA Δ1-HA Δ-HA7

Anti-HA

60
45
35
25

	Cell Lysate	Secretion
	Mock CD4 WT CD4 ΔTM	Mock CD4 WT CD4 ΔTM

Anti-CD4

cis-Golgi

Anterograde transport

Lack of export signal

ER

COOH

UGT2B7